Biochemical and Biophysical Research Communications 452 (2014) 1098–1103

Contents lists available at ScienceDirect

Biochemical and Biophysical Research Communications

journal homepage: www.elsevier.com/locate/ybbrc

Structural insights into the histidine trimethylation activity of EgtD from *Mycobacterium smegmatis*

Jae-Hee Jeong [1], Hyung Jin Cha [1], Sung-Chul Ha, Catleya Rojviriya, Yeon-Gil Kim *

Pohang Accelerator Laboratory, Pohang University of Science and Technology, Pohang, Kyungbuk 790-784, Republic of Korea

ARTICLE INFO

Article history:
Received 31 August 2014
Available online 22 September 2014

Keywords:
Methyltransferase
S-adenosyl-L-methionine
Antioxidant
Mycobacterium smegmatis
Crystal structure

ABSTRACT

EgtD is an *S*-adenosyl-L-methionine (SAM)-dependent histidine *N,N,N*-methyltransferase that catalyzes the formation of hercynine from histidine in the ergothioneine biosynthetic process of *Mycobacterium smegmatis*. Ergothioneine is a secreted antioxidant that protects mycobacterium from oxidative stress. Here, we present three crystal structures of EgtD in the apo form, the histidine-bound form, and the *S*-adenosyl-L-homocysteine (SAH)/histidine-bound form. The study revealed that EgtD consists of two distinct domains: a typical methyltransferase domain and a unique substrate binding domain. The histidine binding pocket of the substrate binding domain primarily recognizes the imidazole ring and carboxylate group of histidine rather than the amino group, explaining the high selectivity for histidine and/or (mono-, di-) methylated histidine as substrates. In addition, SAM binding to the MTase domain induced a conformational change in EgtD to facilitate the methyl transfer reaction. The structural analysis provides insights into the putative catalytic mechanism of EgtD in a processive trimethylation reaction.

1. Introduction

The *S*-adenosyl-L-methionine (SAM)-dependent methyltransferases (MTases) play central roles in a variety of cellular processes, such as biosynthesis, metabolism, cell signaling, and gene regulation in most organisms [1,2]. These enzymes transfer a methyl group from a SAM cofactor to various types of acceptor molecules, including small metabolites, proteins, lipids, and nucleic acids, to methylate the substrate [3]. MTases can be classified into five main classes (I–V) based on the structurally distinct MTase fold, although they catalyze the same methylation reaction [4]. Most known MTases have a class I fold, which consists of a central seven-stranded β-sheet flanked by two layers of α-helices to form an αβα sandwich [2].

Although the class I MTases are characterized by a common fold, they exhibit distinct structural features in SAM and substrate recognition. SAM binds to the spatially equivalent region of the MTase fold through conserved interactions with the GxG motif and an acidic residue, either glutamate or aspartate. The acidic residue forms hydrogen bonds with the hydroxyl groups of the SAM ribose, while the backbone amide N atoms of the GxG motif are hydrogen-bonded to the SAM nucleotide [3]. Except two conserved elements, the interactions of SAM are mediated by different types of residues in different MTases to properly locate the activated methyl group toward a substrate [5]. For substrate recognition, an additional domain might be appended to the SAM-binding MTase domain depending on the property of the substrate. This domain is variable among MTases [2], which is consistent with the fact that these enzymes methylate a variety of distinct substrates. Thus, structural studies on each MTase are necessary to define the catalytic mechanisms of MTases at the molecular level.

EgtD is an *S*-adenosyl-L-methionine (SAM)-dependent *N,N,N*-methyltransferase that is involved in the ergothioneine biosynthetic pathway in *Mycobacterium smegmatis* [6]. Ergothioneine is a secreted antioxidant thought to protect mycobacterium from oxidative stress [7]. Ergothioneine biosynthesis starts with histidine and proceeds through four enzymatic reactions that are mediated by four proteins (EgtD, EgtB, EgtC, and EgtE). EgtD is responsible for the generation of hercynine by trimethylation on the α-nitrogen atom of histidine during ergothioneine synthesis as the first reaction step [6]. To better understand the catalytic mechanism of EgtD, we determined three crystal structures of EgtD: apo-EgtD, EgtD-histidine and EgtD-*S*-adenosyl-L-homocysteine (SAH)-histidine. The structural analysis revealed that EgtD contains the class I MTase fold with an additional substrate binding domain. The structural analysis provides insights into the structural basis for substrate and cofactor recognition and the catalytic mechanism for processive methylation reactions.

* Corresponding author. Fax: +82 54 279 1599.
E-mail address: ygkim76@postech.ac.kr (Y.-G. Kim).
[1] These authors contributed equally to this work.

http://dx.doi.org/10.1016/j.bbrc.2014.09.058
0006-291X/

2. Materials and methods

2.1. Cloning, expression and purification of EgtD

The gene encoding EgtD (UniProt accession No. A0R5M8) from the chromosomal DNA of *M. smegmatis* was amplified by polymerase chain reaction (PCR) with Pfu DNA polymerase. The primers were 5′-ATATCATATGacgctctcactggccaactac-3′ (forward) and 5′-ATATCTCGAGccgcaccgccagcgacaac-3′ (reverse), which contain an NdeI and XhoI site, respectively (underlined). The PCR product was subcloned into the pET30a vector (Novagen) to generate an expression plasmid encoding the full-length *EgtD* gene with a C-terminal His_6-tag. The *EgtD* gene insertion was confirmed by DNA sequencing. The resulting expression vector, pET30a:*EgtD*, was used to transform *Escherichia coli* B834(DE3) cells, which were then grown at 310 K in Luria-Bertani medium containing 100 μg ml^{-1} kanamycin until the OD_{600} reached approximately 0.8. After induction with 0.5 mM isopropyl-β-D-thiogalactopyranoside at 310 K for another 6 h, the cells were harvested by centrifugation at 5000*g* at 277 K. The cell pellet was resuspended in ice-cold buffer A (30 mM Tris–HCl, pH 8.0, 0.3 M NaCl), and the cells were lysed by sonication. The lysate was centrifuged at 15,000*g* for 30 min, and the supernatant was loaded onto a Ni-NTA resin column (Qiagen, USA) equilibrated with buffer A. The eluted protein was further purified using a Superdex 200 (GE Healthcare) column equilibrated in 10 mM Tris–HCl, pH 8.0, and 100 mM NaCl. The fractions containing EgtD were pooled and concentrated up to 35 mg ml^{-1}. Aliquots were flash-frozen in liquid nitrogen and stored at 193 K for later use in crystallization experiments. The SeMet-substituted protein was expressed in minimal medium supplemented with SeMet and purified under the same conditions as the wild-type protein. The purity of the protein was greater than 95% based on SDS-PAGE analysis (data not shown).

2.2. Crystallization and structure determination

All of the crystals were obtained using the sitting drop vapor diffusion method at 295 K by mixing and equilibrating 2 μl of each of protein solution and a precipitant solution. Apo-EgtD was crystallized using a precipitant solution containing 4 M ammonium acetate and 0.1 M imidazole-HCl (pH 9.0). The EgtD-histidine form was crystallized in the precipitant solution used for apo-EgtD, but the solution contained 5 mM histidine (Sigma-Aldrich Co.). The EgtD–SAH–histidine complex was crystallized in a different precipitant solution containing 0.1 M Tris–HCl (pH 9.0), 20% PEG 8 K, and 0.05 M $MgCl_2$, 2 mM SAH, and 5 mM histidine. For data collection, the crystals were briefly immersed in their crystallization solution containing an additional 15% (w/v) glycerol and immediately placed in a 100 K nitrogen gas stream. All of the diffraction data were collected on beamline 5C of the Pohang Accelerator Laboratory (PAL, Republic of Korea). To obtain the phase information of the EgtD structure, a single-wavelength anomalous dispersion (SAD) experiment was performed using apo-EgtD crystals obtained from the selenomethionine-substituted protein. Diffraction data were processed using the *HKL2000* package [8]. *Phenix* was used to locate the Se sites in the apo-EgtD crystal and produced a solvent-flattened map [9]. Model building and refinement of the apo-EgtD structure were performed using *Coot* [10] and *Phenix* [9], respectively. The structures of EgtD-histidine and EgtD-SAH-histidine were determined by the molecular replacement method with the program *Phaser* [11] using the structure of apo-EgtD as a search model. The structures were rebuilt and refined in the same manner. The X-ray diffraction and structure refinement statistics are summarized in Table 1.

The atomic coordinates and structure factors for apo-EgtD, the EgtD-histidine complex and the EgtD-SAH-histidine complex have been deposited in the PDB under accession codes 4UY5, 4UY7 and 4UY6, respectively.

3. Results and discussion

The trimethyltransferase EgtD was crystallized in three structural forms: apo-EgtD, the EgtD-histidine complex and the EgtD-SAH-histidine complex (Table 1). The refined EgtD structures represent the entire molecule of EgtD (2–321 residues) and lack

Table 1
Data collection and refinement statistics of EgtD.

	Apo-EgtD (SeMet)	EgtD-histidine	EgtD-SAH-histidine
Data collection			
Space group	$P4_12_12_1$	$P4_1$	$P4_12_12_1$
Cell dimensions			
a, *b*, *c* (Å)	74.6/74.6/139.7	74.5/74.5/139.0	71.0/71.0/125.0
α, β, γ (°)	90/90/90	90/90/90	90/90/90
Wavelength (Å)	0.9795 (peak)	0.9795	0.9795
Resolution (Å)	30–2.0	30–2.3	50–2.0
R_{sym}[a] (%)	12.1 (34.1)[b]	11.2 (32.3)[b]	8.5 (35.7)[b]
$I/\sigma(I)$	39.2 (3.7)	34.0 (3.3)	60.0 (8.6)
Completeness (%)	99.4 (98.4)	96.9 (92.6)	99.8 (99.7)
Redundancy	13.7 (5.7)	5.2 (3.3)	14.5 (11.2)
Structure refinement			
Resolution (Å)	27.1–2.0	29.0–2.3	46.6–2.0
No. of reflections	31,521	33,047	24,320
R_{work}[c]/R_{free}	19.1/24.1	19.3/25.0	18.0/23.4
No. atoms, Protein/Water	2501/82	5062/27	2503/137
R.m.s. deviations			
Bond lengths (Å)	0.008	0.009	0.008
Bond angles (°)	1.06	1.17	1.11
Average *B*-factor (Å^2)	33.2	25.8	32.9
Ramachandran plot			
Favored (%)	91	89.6	93.3
Additional allowed (%)	9	10.2	6.7
Generally allowed (%)	0	0.2	0

[a] $R_{sym} = \Sigma |I_{obs} - I_{avg}|/I_{obs}$, where I_{obs} is the observed intensity of individual reflection and I_{avg} is average over symmetry equivalents.
[b] The numbers in parentheses are statistics from the highest resolution shell.
[c] $R_{work} = \Sigma ||F_o| - |F_c||/\Sigma |F_o|$, where $|F_o|$ and $|F_c|$ are the observed and calculated structure factor amplitudes, respectively. R_{free} was calculated with 5% of the data.

only the first methionine residue and the C-terminal 6-histidine tag. The asymmetric unit of apo-EgtD and the EgtD-SAH-histidine complex contains one molecule, while the asymmetric unit of the EgtD-histidine complex contains two molecules. An analysis of crystal packing and protein interfaces did not support the formation of an oligomer because the largest interaction area with an adjacent molecule is only 705 Å^2, corresponding to only 5% of the total surface area. This result is consistent with the result of size exclusion chromatography, in which EgtD exists as a monomer in solution (data not shown).

3.1. Overall structure of EgtD

EgtD is composed of two distinct domains: the catalytic MTase domain (residues 2–10, 56–197 and 287–321) and the substrate binding domain (residues 11–55 and 198–286) (Fig. 1A). The catalytic MTase domain contains a central eight-stranded β-sheet (β1–6 and β12–13) sandwiched by two layers of α-helices (α3–α4–α5 and α6–α7–α10) (Fig. 1B). The central β-sheet comprises seven parallel β-strands and only one antiparallel strand, β13; the strands are arranged in the order of β1, β4, β3, β2, β5, β6, β13, and β12, indicating that EgtD belongs to the Rossman-like fold of class I MTases with an additional β1 strand [4,5]. Based on homolog searches in the Dali server, the MTase domain shares the highest similarities with the histamine *N*-methyltransferase HNMT (PDB ID 1JQD; RMSD, 3.4 Å for 208 residues) [12].

The substrate binding domain is unique to EgtD as no equivalent fold domain was found in other methyltransferases or in a DALI search of the Protein Data Bank [13]. The domain consists of five β strands (β7–11) and four α-helices (α1–2 and α8–9). The β strands form two anti-parallel β-sheets arranged in an orthogonal manner, and four helices are placed between two β-sheets (Fig. 1A). As observed in many other MTases, the substrate binding domain is formed by two non-contiguous regions (Fig. 1B). The first segment composing two helices (α1–2) is inserted between β1 and α3 of the MTase domain. The second segment composing the other part of the domain is inserted between β6 and α10 of the MTase domain. Thereby, the substrate binding domain is connected to the MTase domain via four loops. This observation further supports that MTases have acquired substrate specificity by the insertion of structural elements at various places in a common ancestral MTase.

3.2. The substrate binding site

The histidine substrate binding pocket is buried deep inside EgtD and is adjacent to the SAM binding site. The imidazole ring of histidine fits into the pocket formed by the residues of Met252, Phe216, Tyr206, Tyr56, Phe47, Ile50 and Thr213 through the van der Waals interactions and hydrogen bonding formations. The two nitrogen atoms, ND1 and NE2, of the imidazole ring form hydrogen bonds with the side chain of Glu282 and a water molecule anchored by the side chain of Thr213 and the main chain of Ala205, respectively. The carboxylate group of histidine forms an extensive hydrogen bonding network with the side chains of Tyr56, Tyr206, Ser284 and Asn166, while the α-amino group of histidine forms only one hydrogen bond with the side chain oxygen of Asn166 (Fig. 2A). In brief, EgtD mainly interacts with the substrate by recognizing the imidazole ring and carboxylate group rather than the amino group part. Thereby, EgtD can accommodate not only histidine but also the (mono-, di-) methylated histidines as substrates during the processive methylation reactions.

A conformational change upon histidine binding is suspected because histidine is not accessible from the solvent to the substrate binding pocket in the EgtD-histidine form (Fig. 2B), although the superimposition of the EgtD-histidine structure on the apo-EgtD structure did not show a significant difference in the conformation with an root-mean-square deviation (RMSD) of 0.38 Å. Interestingly, the substrate binding pocket of the apo-EgtD structure is occupied by imidazole and acetate molecules, which are used in the crystallization solution. The interaction mode of the bound imidazole and acetate molecules highly resembles that of histidine (Fig. 2C). Therefore, we could not exclude the possibility that the binding of histidine causes rigid body movement between the two domains in the physiological environment where the imidazole and acetate should not occupy the histidine binding pocket because of their low concentration. A conformational change would be induced by forming hydrogen bonds between histidine

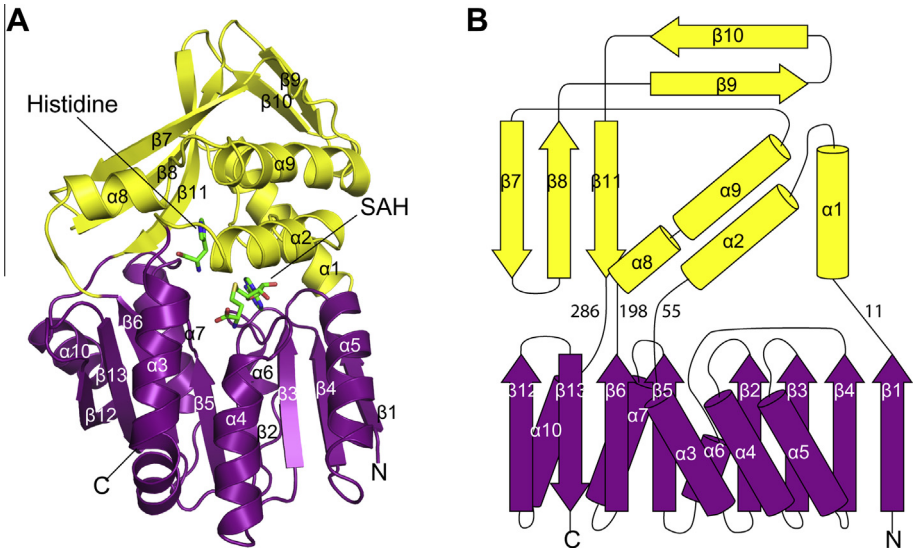

Fig. 1. The overall structure of EgtD from *M. smegmatis*. (A) Ribbon representation of the EgtD-SAH-histidine structure. The MTase and substrate binding domains of EgtD are shown in purple and yellow, respectively. Cofactor and histidine molecules bound to the active site are presented as a stick model. In this orientation, the substrate binding domain is at the top, and the MTase domain is at the bottom. (B) Topology diagram of EgtD. The secondary structural elements are colored as in A. The inclusive numbers indicate the residues constituting the substrate binding domain. (For interpretation of the references to colour in this figure legend, the reader is referred to the web version of this article.)

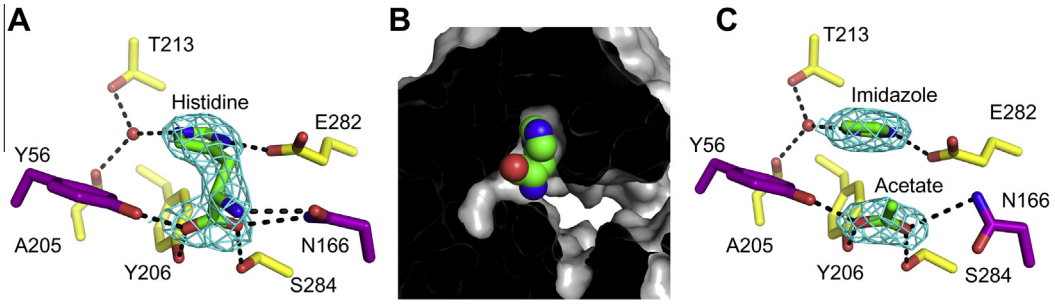

Fig. 2. Substrate binding site of EgtD. (A) Histidine binding to the substrate binding pocket of EgtD. The final 2Fo-Fc electron density for histidine was contoured at the 1.5 σ level. The residues that interact with the ligand by forming hydrogen bonds are depicted as a stick model. The residues are colored as described in the legend of Fig. 1. A water molecule is shown as a red sphere, and hydrogen bonds are indicated as black dashed lines. (B) A cutaway view of the substrate binding pocket. Histidine is presented as a sphere model. (C) Imidazole and acetate molecules at the substrate binding pocket. The map and interacting residues are presented at the same orientation as in A. (For interpretation of the references to colour in this figure legend, the reader is referred to the web version of this article.)

and the MTase domain. Indeed, two residues, Tyr56 and Asn166, from the MTase domain contribute to substrate binding by forming hydrogen bonds with the carboxylate group of histidine as described above. The apo-form of EgtD in cells will have an open conformation for the easy access of the substrate into the substrate binding pocket.

3.3. SAM/SAH binding

The SAM binding site is located on top of the ß-sheet of the MTase domain and just beneath the substrate binding domain. The electron density of the cofactor SAH, a demethylated byproduct of SAM, is well defined and allows a straightforward modeling of SAH into the SAM binding site in the EgtD-SAH-histidine structure. The bound SAH molecule adopts the extended form observed in most other class I MTases, with the O4′-C4′-C5′-S^{δ} torsion angle of ~180°. The SAM molecule will have identical conformation and interactions due to the high degree of chemical similarity with SAH.

The SAM binding groove contains a few unusual features, but it is similar to those observed in other methyltransferases [12,14,15] (Fig. 3A). The homocysteine portion of SAH extends along the conserved GxG motif (residues 86–88) between the β2 strand and α4 helix. The carboxylate group of SAH forms an electrostatic interaction with Lys92 and a water-mediated hydrogen bond with Thr59. The amino group of SAH forms a hydrogen bonding network in direct interaction with the carbonyl oxygen atom of Gly86, one of the glycines in the GxG motif but also an indirect interaction with the main chain of Leu160 and the side chain of Thr163 through water molecules. The ribose moiety forms hydrogen bonding interactions via the two hydroxyl groups to the side chain of Asp113 at the end of ß3 strand and to a water molecule anchored by the side chain of Ser44. This acidic residue (Glu or Asp) is invariantly conserved among the MTases for the recognition of the ribose moiety of SAM/SAH [5]. The adenine ring forms a number of hydrophobic interactions with the residues Val114, Lys36 and Tyr39 and is stacked with the side chain of Phe142. In addition, the side chain of Asp141 and the main chain nitrogen atom of

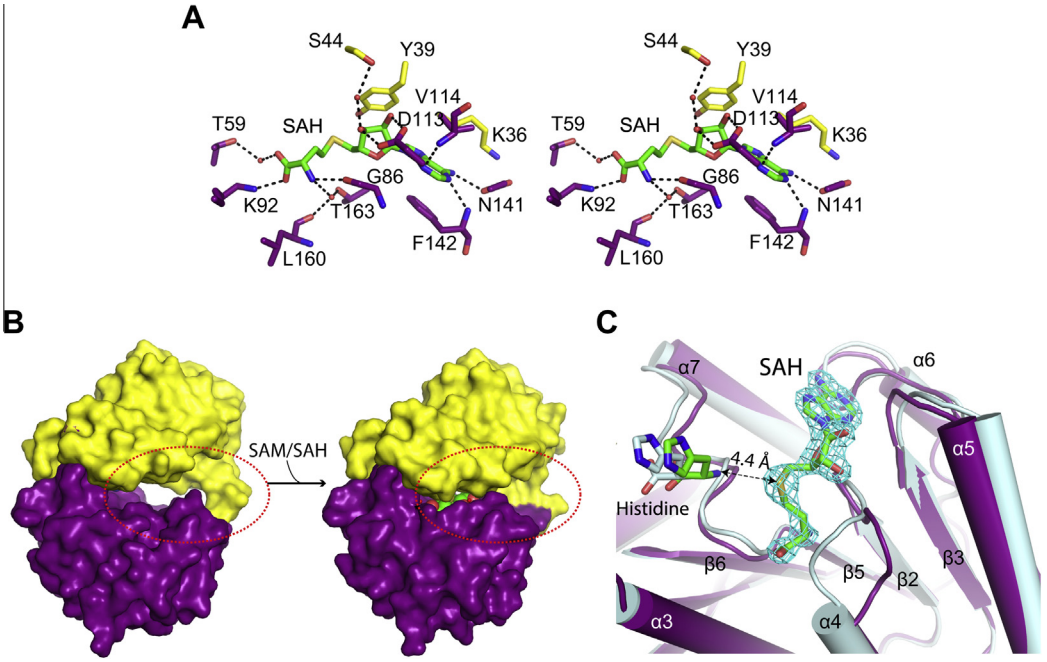

Fig. 3. SAM/SAH binding of EgtD. (A) Stereoview of the cofactor binding site, showing the residue interactions with the SAH molecule. (B) Overall conformational change of EgtD induced by SAH binding. The MTase domains of the EgtD-histidine (left) and EgtD-SAH-histidine (right) structures were superposed, and two structures are presented as a surface model in the same orientation. The region showing considerable structural changes is highlighted with a dashed circle. The bound SAH molecule is shown as a sphere model. (C) Comparison of the MTase domains of EgtD-histidine (gray) and the EgtD-SAH-histidine complex (purple). The final 2Fo-Fc electron density for SAH was contoured at the 1.5 σ level. SAH is shown as a stick model. The distance between the nitrogen atom of histidine and the sulfur atom of SAH in the EgtD-SAH-histidine structure is indicated. (For interpretation of the references to colour in this figure legend, the reader is referred to the web version of this article.)

Phe142 form hydrogen bonds to the N6 amino group and the N1 atom on the adenine ring, respectively.

The SAM molecule could be modeled in the cofactor binding site by adding a C^{ε} atom to the S^{δ} of the SAH molecule with appropriate stereochemistry using the known structure of SAM. The methyl group is in van der Waals contact with the side chains of Thr39, Phe47 and Thr163. The modeled C^{ε} atom is located close to the α-nitrogen atom of histidine at a distance of 2.55 Å. Interestingly, the phenyl group of Phe47 faces the S^{δ} atom of SAH at a distance of 3.6 Å. This contact will contribute to the stabilization of the cation of the S^{δ} atom through a cation–π interaction when the SAM molecule binds to this groove.

3.4. Conformational change induced by SAH/SAM binding

To examine the conformational change induced by SAH binding to EgtD, the EgtD-SAH-histidine structure was superimposed upon the structures of apo-EgtD and EgtD-histidine with RMDS values of 1.56 Å and 1.49 Å, respectively. The conformational change of EgtD upon SAH/SAM binding is more apparent when the MTase domain is used for the superposition of the structures. The superimposed MTase domains exhibit RMSDs between equivalent C_{α} atoms of 0.25 Å, whereas the non-superimposed substrate binding domain shows a 7.0 Å displacement at the beginning of the α1 helix, indicating the flexibility between the two domains (Fig. 3B).

Although the MTase domain did not show significant conformational changes upon SAH binding, local conformational changes to accept a SAH molecule have been observed (Fig. 3C). The most conspicuous regions include the loop between the β2 strand and α4 helix, α5 helix, and β5–α7 loop. Most of the residues in these regions are involved in the formation of the SAH/SAM binding groove. Importantly, these local conformational changes on the MTase domain seem to induce rigid body movement of the substrate binding domain because there are only marginal interactions between the SAH molecule and residues from the substrate binding domain. The inter-domain movement causes the α-amine group of histidine to move forward to the S^{δ} atom of SAH with an approximate 1.7 Å distance. In this configuration, the α-amino group of histidine is located 4.4 Å from the S^{δ} atom of SAH. Therefore, the flexibility of the two domains should be critical to accomplish the reaction cycle to allow access of the substrate and release of the product.

3.5. Putative catalytic mechanism of EgtD

The catalytic mechanism of SAM-dependent methyltransferases is known to proceed by a classic SN2 reaction involving inversion of the stereochemistry for the methyl group of SAM [16]. This mechanism requires a linear arrangement of the amino nitrogen (N) nucleophile, the methyl carbon atom (C^{ε}), and the sulfonium atom (S^{δ}) of SAM in the transition state of the reaction. In addition, three chemical mechanisms have been proposed for catalyzing the transmethylation reaction: (i) proximity and orientation effects, (ii) general acid/base-mediated catalysis, and (iii) metal-dependent mechanisms [1]. Based on the structural analysis, we propose that EgtD catalyzes the methyl transfer reaction by a proximity and orientation effect. The modeled SAM shows that the three atoms (S^{δ}–C^{ε}–N) are arranged at an angle of 164° with a 2.55 Å distance between the nitrogen and methyl group. This distance would be suitable for methyl transfer to occur directly between the donor SAM methyl group and the acceptor α-nitrogen atom of histidine. In addition, the conformational flexibility between the two domains and/or molecular vibration can lead a collision between the lone pair of electrons from the nitrogen and the methyl group so that a SN2 methyl transfer reaction occurs (Fig. 4).

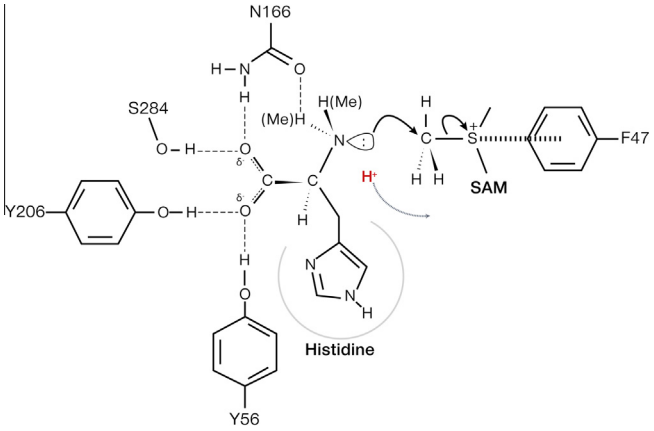

Fig. 4. Scheme of the proposed speculative catalytic mechanism of EgtD. The α-amino nitrogen of histidine is aligned for a direct in-line SN2 nucleophilic attack by forming hydrogen bonding interactions with the depicted residues. The positively charged sulfonium ion of SAM will be stabilized by the charge–π interaction with Phe47. The lone pair of electrons from the nitrogen will be obtained after a proton loss to solvent, which is indicated as a red letter and a dashed arrow during the processive methylation reactions. (For interpretation of the references to colour in this figure legend, the reader is referred to the web version of this article.)

In a precatalytic state, histidine would bind first to the substrate binding pocket of apo-EgtD before SAM binding because the entrance of the histidine binding pocket is nearly occluded by the SAH molecule (Fig. 3B). The hydrogen bonding interaction between the α-amino group of histidine and the $O^{\delta 1}$ of Asn166 will orient the lone pair of electrons from the α-nitrogen to point toward the incoming methyl group. Subsequently, the SAM molecule will bind to the cofactor groove as described above. Especially, the cation–π interaction between the positively charged sulfonium ion of SAM and the phenyl group of Phe47 will facilitate the SN2 reaction. Furthermore, SAM binding induces rigid body movement of the two domains, bringing the acceptor α-amino group of histidine into close proximity to the reactive methyl group of SAM at a distance of 2.55 Å. The absence of a general base around the substrate implies that the lone pair of electrons in the α-amino group can be readily generated by water solvent because the pK_a value is approximately ~8.0. After the first methyl transfer reaction, the deprotonation of the amine group will occur by a solvent-based mechanism, as well as after the release of SAH as simulated in other methyltransferases [17,18]. In addition, the rotational movement of the amine group after the first and/or second methylation reactions should be necessary for the processive catalytic mechanism as observed in other MTases [19,20]. As described above, the α-amino group of histidine is restricted by only one hydrogen bond with Asn166, which might allow the rotation of the methylated amine group away from the line of nucleophilic attack. Once the second round of methyl transfer reaction is completed, the bulky tertiary amine groups will lose the hydrogen bond with Asn166, and eventually the side chain of Asn166 should have a different conformation to avoid steric hindrance with the methyl group. During the positioning of the di-methyl groups in the substrate binding pocket, the lone pair of electrons of the amine group will be arranged in the line of nucleophilic attack. After the third methylation reaction, the interactions between the hercynine product and EgtD will be destabilized because no space is available to accommodate the third transferred methyl group, thereby it will be released from the substrate binding site.

Conflict of interest

The authors declare that they have no conflict of interest.

Acknowledgments

This research was supported by Basic Science Research Program through the National Research Foundation of Korea (NRF) funded by the Ministry of Education, Science and Technology (Grant 2011-0007201).

References

[1] D.K. Liscombe, G.V. Louie, J.P. Noel, Architectures, mechanisms and molecular evolution of natural product methyltransferases, Nat. Prod. Rep. 29 (2012) 1238–1250.
[2] J.L. Martin, F.M. McMillan, SAM (dependent) I AM: the *S*-adenosylmethionine-dependent methyltransferase fold, Curr. Opin. Struct. Biol. 12 (2002) 783–793.
[3] A.W. Struck, M.L. Thompson, L.S. Wong, J. Micklefield, *S*-adenosyl-methionine-dependent methyltransferases: highly versatile enzymes in biocatalysis, biosynthesis and other biotechnological applications, ChemBioChem 13 (2012) 2642–2655.
[4] H.L. Schubert, R.M. Blumenthal, X. Cheng, Many paths to methyltransfer: a chronicle of convergence, Trends Biochem. Sci. 28 (2003) 329–335.
[5] R. Gana, S. Rao, H. Huang, C. Wu, S. Vasudevan, Structural and functional studies of *S*-adenosyl-L-methionine binding proteins: a ligand-centric approach, BMC Struct. Biol. 13 (2013) 6.
[6] F.P. Seebeck, In vitro reconstitution of *Mycobacterial ergothioneine* biosynthesis, J. Am. Chem. Soc. 132 (2010) 6632–6633.
[7] C. Sao Emani, M.J. Williams, I.J. Wiid, N.F. Hiten, A.J. Viljoen, R.D. Pietersen, P.D. van Helden, B. Baker, Ergothioneine is a secreted antioxidant in *Mycobacterium smegmatis*, Antimicrob. Agents Chemother. 57 (2013) 3202–3207.
[8] Z. Otwinowski, W. Minor, Processing of X-ray diffraction data collected in oscillation mode, Macromol. Crystallogr. A 276 (1997) 307–326.
[9] P.D. Adams, P.V. Afonine, G. Bunkoczi, V.B. Chen, I.W. Davis, N. Echols, J.J. Headd, L.W. Hung, G.J. Kapral, R.W. Grosse-Kunstleve, A.J. McCoy, N.W. Moriarty, R. Oeffner, R.J. Read, D.C. Richardson, J.S. Richardson, T.C. Terwilliger, P.H. Zwart, PHENIX: a comprehensive python-based system for macromolecular structure solution, Acta Crystallogr. D Biol. Crystallogr. 66 (2010) 213–221.
[10] P. Emsley, K. Cowtan, Coot: model-building tools for molecular graphics, Acta Crystallogr. D Biol. Crystallogr. 60 (2004) 2126–2132.
[11] A.J. McCoy, R.W. Grosse-Kunstleve, P.D. Adams, M.D. Winn, L.C. Storoni, R.J. Read, Phaser crystallographic software, J. Appl. Crystallogr. 40 (2007) 658–674.
[12] J.R. Horton, K. Sawada, M. Nishibori, X. Zhang, X. Cheng, Two polymorphic forms of human histamine methyltransferase: structural, thermal, and kinetic comparisons, Structure 9 (2001) 837–849.
[13] L. Holm, C. Sander, Protein structure comparison by alignment of distance matrices, J. Mol. Biol. 233 (1993) 123–138.
[14] J. Bauer, G. Ondrovicova, L. Najmanova, V. Pevala, Z. Kamenik, J. Kostan, J. Janata, E. Kutejova, Structure and possible mechanism of the CcbJ methyltransferase from *Streptomyces caelestis*, Acta Crystallogr. D Biol. Crystallogr. 70 (2014) 943–957.
[15] O. Cakici, M. Sikorski, T. Stepkowski, G. Bujacz, M. Jaskolski, Crystal structures of NodS N-methyltransferase from *Bradyrhizobium japonicum* in ligand-free form and as SAH complex, J. Mol. Biol. 404 (2010) 874–889.
[16] D. O'Hagan, J.W. Schmidberger, Enzymes that catalyse S(N)2 reaction mechanisms, Nat. Prod. Rep. 27 (2010) 900–918.
[17] X. Zhang, T.C. Bruice, Product specificity and mechanism of protein lysine methyltransferases: insights from the histone lysine methyltransferase SET8, Biochemistry 47 (2008) 6671–6677.
[18] X. Zhang, T.C. Bruice, Enzymatic mechanism and product specificity of SET-domain protein lysine methyltransferases, Proc. Natl. Acad. Sci. U.S.A. 105 (2008) 5728–5732.
[19] X. Cheng, X. Zhang, Structural dynamics of protein lysine methylation and demethylation, Mutat. Res. 618 (2007) 102–115.
[20] X. Zhang, Z. Yang, S.I. Khan, J.R. Horton, H. Tamaru, E.U. Selker, X. Cheng, Structural basis for the product specificity of histone lysine methyltransferases, Mol. Cell 12 (2003) 177–185.